2022 IEEE International Symposium on Radio-Frequency Integration Technology (RFIT)

August 29 - 31, 2022, Busan, Korea

A Compact Mm-Wave Multi-Band VCO Based on Triple-Mode Resonator for 5G and Beyond

2022 IEEE International Symposium on Radio-Frequency Integration Technology (RFIT) | 978-1-6654-6649-3/22/$31.00 ©2022 IEEE | DOI: 10.1109/RFIT54256.2022.9882424

Mohammad Chahardori
Dept of Electrical Engineering and Computer Science
Washington State University
Pullman, USA
Mohammad.chahardori@wsu.edu

MD Aminul Hoque
Dept of Electrical Engineering and Computer Science
Washington State University
Pullman, USA
mdaminul.hoque@wsu.edu

Mohammad Ali Mokri
Dept of Electrical Engineering and Computer Science
Washington State University
Pullman, USA
m.mokri@wsu.edu

Deukhyoun Heo
Dept of Electrical Engineering and Computer Science
Washington State University
Pullman, USA
dheo@wsu.edu

We present a low phase noise four-core triple-band voltage controlled-oscillator (VCO) with reconfigurable oscillator cores and multi-mode resonator. By activation/deactivation of oscillator cores and change of resonator impedance in three modes of operations, the proposed VCO provides complete freedom in selecting the resonance frequency for three operation bands in the mm-wave range. The proposed four-core triple-band VCO is implemented in a 65 nm CMOS process using a compact high-Q triple-mode resonator. The VCO oscillation frequencies center at 19, 28, and 38 GHz while providing good phase noise and low power consumption in all bands. Measured results show the total frequency tuning range (FTR) of 38.5% while the PN at 1MHz offset varies from -100.3 dBc/Hz to -106.06dBc/Hz resulting in an excellent FoM_T of 199.8 dBc/Hz.

***Keywords*— Voltage-controlled oscillators, 5G communication, multi-band, low phase noise, low power consumption.**

I. INTRODUCTION

In applications such as mm-wave 5G, due to the wide separation in the allocated frequency bands and the stringent phase noise (PN) requirements in LO generation block, multi-band VCOs can provide exceptional performance compared to wideband VCOs covering the whole 5G band. Multi-mode VCOs have shown promising performance by providing different resonance frequencies from a single resonator without using multiple separate VCOs or passive components with series switches [1-4]. In [1], a dual-mode VCO is demonstrated based on a high Q dual-mode inductor to provide high performance at two different mm-wave resonance frequencies. Avoiding series switches in the dual-mode inductor in [1] to change the modes of operation enables both PN reduction and frequency tuning range (FTR) extension. However, the method was limited to only two modes of operation with small frequency separation making it hard to be used to design a dual-band VCO with a large frequency separation such as 28GHz and 38GHz required in 5G mm-wave applications. A triple-band VCO based on a multi-mode inductor was introduced in [2] with a small form factor. However, in this VCO, a conventional capacitor bank with series switches in the resonator is used to provide the third frequency band. These series switches reduce the resonator Q, compromising frequency separation between bands and PN in the third frequency band. The triple-mode VCOs [3]-[4] provide low PN and a very wide tuning range by leveraging configurable coupled oscillator cores and multi-mode inductors. However, the multi-mode inductors consist of two different metal layers introducing a lower Q due to the lower thin metal layer. In addition, coupling between different metal layers reduces the self-resonance frequency and limits the maximum frequency of operation.

This paper presents a new four-core triple-band VCO, which leverages the benefits of a reconfigurable structure and a compact single metal-layer dual-path inductor and mode switching capacitors for band selection. As a result, the new four-core structure allows the VCO to operate at three different modes of operation without increasing chip size and sacrificing the PN performance compared to prior multi-mode VCOs.

II. PROPOSED TRIPLE-BAND FOUR-CORE VCO

Fig. 1 shows the proposed triple-band VCO consisting of four reconfigurable class-D oscillator cores. Each core includes a cross-coupled transistor pair to provide the required negative gm for oscillation and a tail transistor, which is used as a switch to enable or disable the core in different modes of operation coupled with a compact high-Q triple-mode resonator. Fig. 1 also demonstrates the structure of the proposed triple-mode resonator with parallel mode selection switches. The resonator is a four-port network with high-Q dual-path inductors and mom cap capacitors (C_1 and C_2) in parallel with all four output ports. The resonator also includes three pairs of switches for selecting the operation modes and frequency bands of the VCO. This new four core structure for triple-band VCO compared to the prior triple-band VCO with band selecting capacitor banks [4] removes the series switches in band-select capacitor banks and puts the switches in the tail of cores to change the band of operation. Since the tail switches of cores are ON only when the cores are active, they act as tiny resistors connected to the ground. Thus, they do not contribute to the VCO output-referred noise, and as a result, they do not affect the PN performance of the VCO.

A. Triple-Band VCO Operation

The operation of the proposed triple-band VCO can be described in three different modes of operation. In the first mode of operation (the lower frequency band), core switches

S_A and resonator mode-selection switches S_X in Fig.1 are ON, and all other switches are OFF. Consequently, the two cross-coupled cores A are active, and the two cross-coupled cores B are disabled. Since S_X switches in the resonator are ON and act as a tiny resistor, the shorter loop of the dual-path inductor is a short circuit, and the four-port inductor work as two larger inductors (L_1), including only larger loops at the output of cores A. At the same time, since S_X switches are on the capacitors C_2 are short circuit and only capacitors C_1 are seen at the output resonator. In this case, the resonator circuit just consists of the inductor of a larger loop and capacitors of C_1, which has a larger value compared to C_2. The resonance frequency in this mode can be calculated as:

$$\omega_{Lower\_Band} = \frac{1}{\sqrt{L_1 \cdot C_1}} \quad (1)$$

In equation (1), the parasitic capacitors have been ignored for simplicity. In the second mode of operation (the higher frequency band), core switches S_B and resonator mode-selection switches S_Y are ON, and all other switches are OFF. The two cross-coupled cores B are activated, and the two cross-coupled cores A are disabled. In this operation, since the switches S_Y are ON, the shorter loop of the dual-path inductor is also excited and contribute as the resonator inductors seen at the outputs of the four-port network. Due to the supply connection to the dual-path inductor in Fig. 2, the larger loop is not short in this mode of operation, and it appears as a parallel inductor at the resonator output as well. Thus, in this mode of operation the resonator includes both shorter loop inductors L_2 in parallel to larger loop inductors L_1 at the output of cores B. On the other hand, since S_Y switches are ON in this mode, the capacitors C_1 are short circuit, and only capacitors C_2 are seen at the output resonator. In this case, the resonator circuit consists of the two inductors in parallel and capacitors of C_2, which has a smaller value compared to C_1. The resonance frequency in this mode can be calculated as:

$$\omega_{Higher\_Band} = \frac{1}{\sqrt{(L_{1||}L_2) \cdot C_2}} \quad (2)$$

In the third mode of operation (the middle band), core switches S_A, S_B, and resonator mode-selection switches S_Z are ON, and S_X and S_Y are OFF. The activation of S_A and S_B switches results in all four cores A and B being active and simultaneously coupled. On the other hand, capacitors C_1, C_2 and both loops of the inductor are connected to the resonator output. The output resonator includes a parallel combination of C_1, C_2, L_1, and L_2. The resonance frequency in this mode is:

$$\omega_{Middle_{Band}} = \frac{1}{\sqrt{(L_{1||}L_2) \cdot (C_1 + C_2)}} \quad (3)$$

B. Triple-band VCO Stability

The turn-on resistance (R_{ON}) of the mode selection switches S_X, S_Y and S_Z plays a significant role in the stable operation of the triple-band VCO. Without mode selection switches in Fig. 2, the resonator impedance at the VCO outputs generates two separate peaks in amplitude and three zero-crossing points in phase in each mode of operation. Consequently, the VCO can oscillate at either peak frequencies or both frequencies. Sufficiently small R_{ON} is required to avoid oscillation due to the zero-crossing phase at undesired frequency [1].

In Fig. 2, the simulated magnitude and phase of resonator impedance are shown in three different operation modes for different R_{ON}. This plot shows the maximum acceptable R_{ON} in each band to eliminate the unwanted oscillation. Fig. 2 shows that by selecting switch transistors' R_{ON} around 50 **Ω**, the oscillator provides stable oscillation in all three bands of operation. Since the switch has a small size, it does not add considerable parasitic capacitors to the resonator.

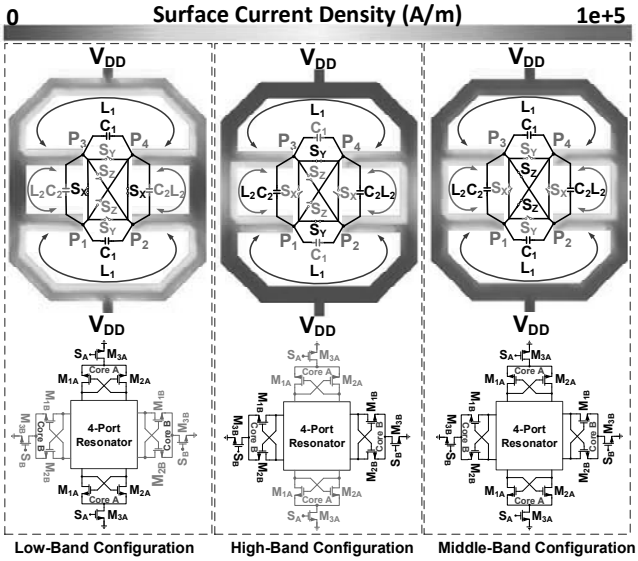

Fig. 1. Configuration of cores and resonator in three operation modes and the dual-path inductor surface current density in each mode.

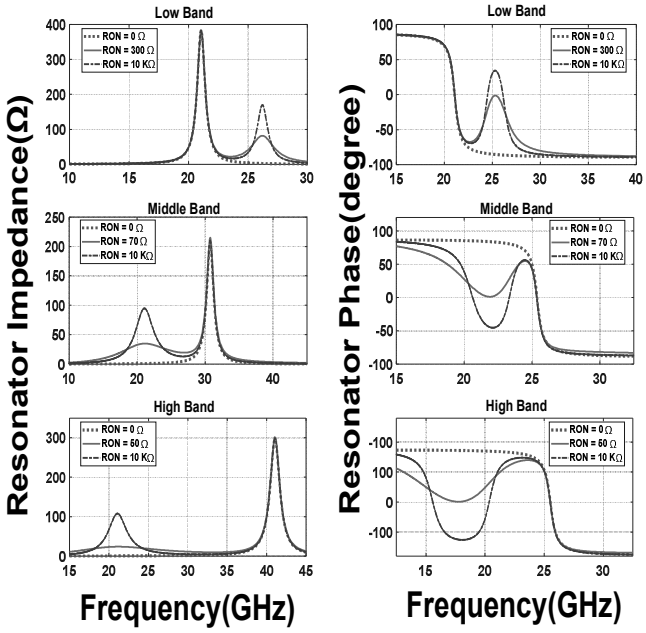

Fig. 2. Simulated resonator impedance in three operation modes for different values of mode switches R_{ON}.

III. EXPERIMENTAL RESULTS

The proposed four-core triple-band VCO was fabricated in a 65nm CMOS process targeting three different frequency bands corresponding to uplink and downlink of satellite communication and two mm-wave 5G standards. A micrograph of the fabricated chip is shown in Fig. 3. The whole oscillator without pads occupies a small silicon area of 0.063 mm2 (250 µm × 250 µm). This chip area is similar to a single band VCO with a coupled resonator since all the active and passive

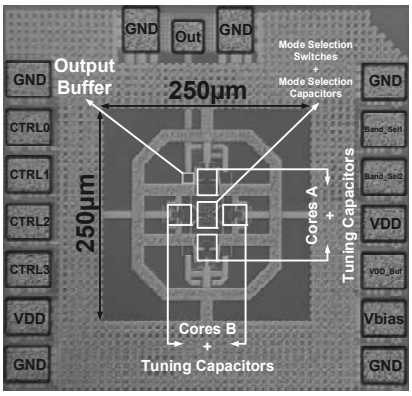

Fig. 3. Die micrograph.

components used in main cores and resonator are placed inside the inductor structure. Thus, the total size of VCO is defined just by inductor size, which is defined mainly by the maximum value of the inductor to cover lower frequency band. Small varactors and 4-bit capacitor banks were connected in parallel with the fixed capacitors C_1 and C_2 to provide fine frequency tuning in each band. These small capacitor banks do not degrade the VCO performance during the band selection since they do not affect the modes of operation.

The VCO provides the best PN at a supply voltage adjusted between 0.4V to 0.5V in different bands when a 1.2V is used for the switches and logic circuits. An on-chip open-drain buffer connected to output port P3 is employed to take out the VCO output in all three frequency bands.

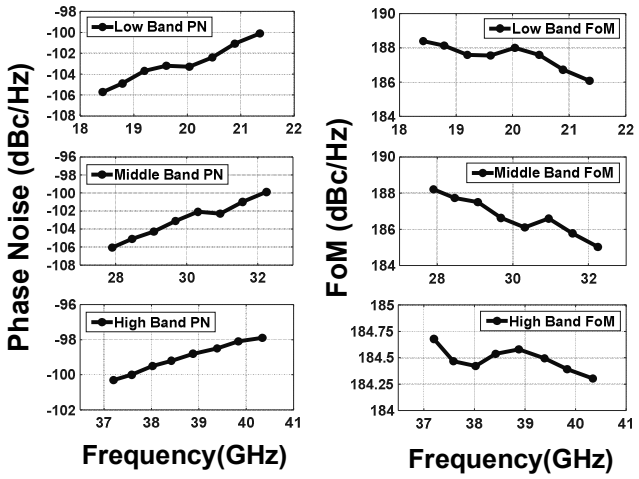

Fig. 4. Measured PN and FoM of the VCO at 1 MHz offset frequency

Fig. 4 demonstrates the measured PN and FoM across the tuning range at 1MHz frequency offset where the PN is not affected by the noise floor of measurement setup. Fig.4 also shows the tuning ranges in the low-, middle-, and high-frequency bands are 18.42-21.36 GHz, 27.9-32.25 GHz, and 37.2-40.34 GHz, corresponding to a fractional tuning range (FTR) of 14.8%, 14.5%, and 8.1%, respectively. The PN at 1 MHz offset varies from -97.9 dBc/Hz to -106.06 dBc/Hz, resulting in the FoM variation of 184.3 dBc/Hz-188.4 dBc/Hz over three different bands. Table. 1 summarizes the measurement results and compares the VCO performance with state-of-the-art VCOs in a similar frequency range. The proposed K-Ka band VCO has achieved very low phase noise and a total FTR of 38.4% provided by the high-Q and compact triple-mode resonator, resulting in excellent FoMT from 195.74 dBc/Hz to 199.83 dBc/Hz.

TABLE. I. PERFORMANCE SUMMARY AND COMPARISON WITH STATE-OF-THE-ART WIDEBAND VCOS IN MM-WAVE FREQUENCY RANGE.

Referenced	This work	[2] IMS'20	[3] ISSCC'21	[4] CICC'21
Technology	65nm CMOS	65nm CMOS	65nm CMOS	65nm CMOS
Frequency (GHz)	19/28/38	19/28/36	52.4 ~ 60.4	8.2 ~ 21.5
FTR (%)	38.4	33.6	14.2	89.6
Power (mW)	1.8 ~ 5	2.4 ~ 4.7	22.5 ~ 23.6	4 ~ 6
PN @1MHz (dBc/Hz)	-100 ~ -107	-101 ~ -108	-102 ~ -105	-94 ~ -108
FoM(1)@1MHz (dBc/Hz)	184 ~ 188	185 ~ 188	182 ~ 187	171 ~180
FoM_T(2)@1MHz (dBc/Hz)	196 ~ 200	195 ~198	185 ~ 189	190 ~199
Core area (mm2)	0.063	0.088	0.032	0.125

(1) $FoM = |PN| + 20\log_{10}(f_0/\Delta f) - 10\log_{10} P_{DC}(mW)$ (2) $FoMT = FoM + 20\log_{10}(FTR[\%]/10)$

ACKNOWLEDGMENT

This work was supported in part by the Center for Design of Analog-Digital Integrated Circuits (CDADIC), in part by Semiconductor Research Corporation (SRC) and in part by NSF under Awards 1955306, 1705026 and 2030159.

REFERENCES

[1] Y. Peng, J. Yin, P.-I. Mak, and R. P. Martins, "Low-Phase-Noise Wideband Mode-Switching Quad-Core-Coupled mm-wave VCO Using a Single-Center-Tapped Switched Inductor," *IEEE J. Solid-State Circuits*, vol. 53, no. 11, pp. 3232–3242, Nov. 2018.

[2] M. A. Hoque, M. Chahardori, P. Agarwal, M. A. Mokri and D. Heo, "Octave Frequency Range Triple-band Low Phase Noise K/Ka-Band VCO with a New Dual-path Inductor," IEEE/MTT-S International Microwave Symposium (IMS), USA, 2020, pp. 341-344,

[3] H. Jia, W. Deng, P. Guan, Z. Wang and B. Chi, "A 60GHz 186.5dBc/Hz FoM Quad-Core Fundamental VCO Using Circular Triple-Coupled Transformer with No Mode Ambiguity in 65nm CMOS," IEEE International Solid- State Circuits Conference (ISSCC), 2021, pp. 1-3.

[4] W. Deng et al., "An 8.2-to-21.5 GHz Dual-Core Quad-Mode Orthogonal-Coupled VCO with Concurrently Dual-Output using Parallel 8-Shaped Resonator," IEEE Custom Integrated Circuits Conference (CICC), pp. 1-2, 2021.